J Mater Sci (2008) 43:464–468
DOI 10.1007/s10853-007-1954-6

5TH BRAZILIAN MRS MEETING

Luminescence of $SrAl_2O_4:Cr^{3+}$

Ada López · Mariana G. da Silva · Elisa Baggio-Saitovitch · Alexandre R. Camara · Raimundo N. Silveira Jr. · Raul José Mauricio da Fonseca

Received: 30 January 2007 / Accepted: 18 June 2007 / Published online: 19 August 2007

Abstract Samples of $SrAl_2O_4$ and $SrAl_2O_4:Cr^{3+}$ were prepared by mixing the powder materials $SrCO_3$, Al_2O_3, and Cr_2O_3. The crystal structures of the undoped and doped samples were analyzed by X-ray diffraction (XRD) measurements. The diffraction patterns reveal a dominant phase, characteristic of the monoclinic $SrAl_2O_4$ compound and another unknown secondary phase, in small amount, for doped samples. The data were fitted using the Rietveld method for structural refinements and lattice parameter constants (a, b, c, and β) were determined. Luminescence of Cr^{3+} ions in this host is investigated for the first time by excitation and emission spectroscopy at room temperature. Emission spectra present a larger band and a smaller structure associated to the $^4T_2\ (^4F) \rightarrow {}^4A_2\ (^4F)$ and $^2E\ (^2G) \rightarrow {}^4A_2\ (^4F)$ electronic transitions, respectively. The obtained results are analyzed by crystal-field theory and the crystal-field parameter, Dq, and Racah parameters, B and C, are determined from the excitation measurements.

Introduction

The interest in developing new compounds that emit in the visible and near-infrared spectral regions is justified by recent advances in tunable solid-state lasers. In particular, materials doped with transition metal and rare earth ions have been intensively studied due to their inherent tunability and possible applications as signal transmission, display devices, and information storage [1–3]. Recently, new phosphor materials have received a special attention in literature because they present an efficient and intense luminescence, which allows the development of new plasma display panels (PNP) [4–6]. Among the different phosphors, Eu^{2+}-doped $SrAl_2O_4$ is the most investigated compound for the reason that it exhibits a strong persistent luminescence. Likewise, others works have analyzed the optical phenomena originated from different rare earth ions included as dopant in this matrix [7–10]. On the other hand, transition metal ions have been widely used in luminescent materials but there are only few reports about these ions in persistent phosphors [11, 12]. In this case, Cr^{3+} is the most studied 3d ion, mainly due to the strong visible absorption and emission bands observed when it is incorporated in oxide and fluoride hosts [13–16]. The unfilled $3d^3$ electronics shell of the Cr^{3+} ion has a number of low-lying energy levels, among which optical transitions can occur generating luminescent emission. As the 3d electrons are outside of the ion core, the optical spectroscopic properties of the Cr^{3+} ions are directly affected by the static and dynamic properties of their environments and the optical associated spectra are characterized by both sharp and broad emission bands. The sharp transitions occur between levels that do not depend on the crystal field intensity while broad bands are associated to electronic states coupled with host vibrational levels, which considerably depend on crystal field strength. A recent work, proposed by Zhong et al. [11], showed that a persistent phosphorescence is obtained through persistent energy transfer from Eu^{2+} ions to Cr^{3+} ions in $Sr_2Al_6O_{11}$, $SrAl_{12}O_{19}$, and $Sr_4Al_{14}O_{25}$

A. López · M. G. daSilva · E. Baggio-Saitovitch
Centro Brasileiro de Pesquisas Físicas, Rua Dr. Xavier Sigaud, 150, Rio de Janeiro, RJ 22290-180, Brazil

A. López · M. G. daSilva · A. R. Camara · R. N. Silveira Jr. · R. J. M. daFonseca (✉)
DEQ, Instituto de Física, Universidade do Estado do Rio de Janeiro, Rua São Francisco Xavier, 524, sala D-3030, Rio de Janeiro, RJ 20550-013, Brazil
e-mail: rauljose@uerj.br

co-doped systems. In all of these compounds, the emission originated from Cr^{3+} ions was located in the red region, more specifically, about 690 nm. However, up to now, the optical influence of Cr^{3+} ions in the lattice of $SrAl_2O_4$ was not yet investigated. Consequently, the aim of this work is to study for the first time the optical properties of $SrAl_2O_4:Cr^{3+}$ through fluorescence and excitation spectroscopy techniques and to suggest the possible mechanism associated to the observed transitions.

Experimental

Sample preparation and structure determination

Polycrystalline samples of the $Sr(Al_{1-x}Cr_x)_2O_4$ series with $x = 0$ and 0.01 were prepared by conventional solid-state reaction with high purity $SrCO_3$, Al_2O_3, and Cr_2O_3 powders (the undoped sample $x = 0$ was done as a reference). The initial mixture was decomposed at 700 °C in air for the synthesis. After milling and pressing procedures, the material was reacted in flowing Ar at 1,200 °C for 12 h. The X-ray diffraction (XRD) patterns were obtained in a X-Pert PRO (PANalytical) powder diffractometer using CuKα(irradiation ($\lambda = 1.5418$ Å). Data have been collected by step-scanning mode ($10° \leq 2\Theta \leq 50°$) and 2 s counting time at each step at room temperature.

Optical measurements

The optical measurement set-up has basically consisted of two Spex model 1670 monochromators that have been used to select the excitation radiation in the wavelength range from 300 to 800 nm. A 1,000 W Xe lamp (for excitation measurements) and a 150 mW Ar laser were used as light sources and their intensities were modulated by a PAR 191 variable speed chopper. Emission measurements were performed with a 2061 MacPherson spectrometer equipped with a RCA C31034-128 photomultiplier placed at the exit slit of the spectrometer. The output signals were fed into an EGG model 5209 lock-in amplifier connected to a microcomputer. Fluorescence lifetimes were measured with the phase shift experimental technique [17].

Results and discussion

The results of powder XRD measurements are shown in Fig. 1, for (a) $SrAl_2O_4$ and (b) $SrAl_2O_4$:Cr samples. The diffraction patterns reveal a dominant phase, characteristic of the monoclinic $SrAl_2O_4$ compound. However, the presence of a small amount of the unknown secondary

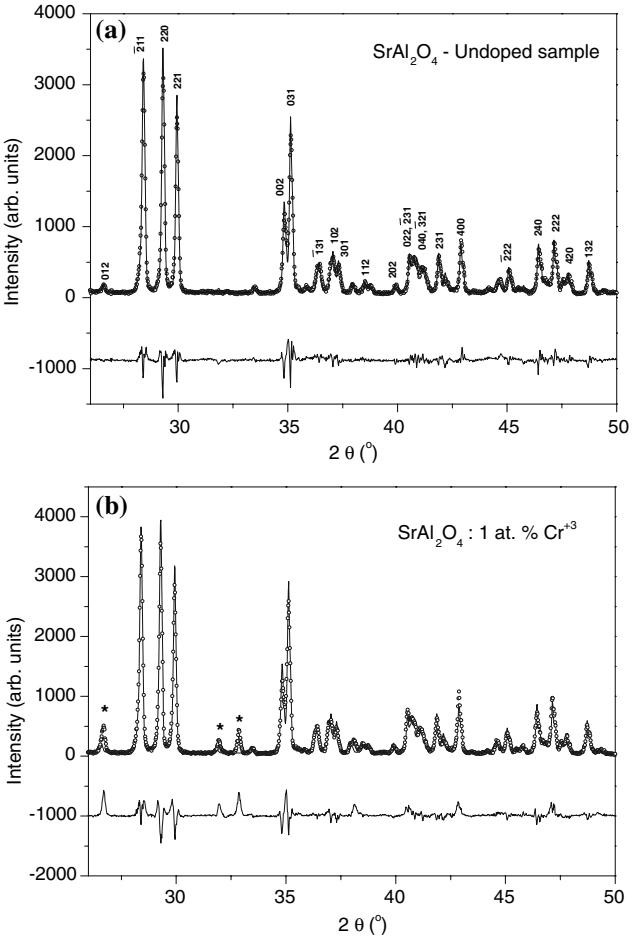

Fig. 1 X-rays diffractograms with Rietveld refinement for the samples (**a**) $SrAl_2O_4$ and (**b**) $Sr(Al_{0.99}Cr_{0.01})_2O_4$. The curve and points are the theoretical and experimental patterns respectively. The bottom curves represent the difference between the theoretical and experimental patterns. The peaks of the unknown secondary phase are indicated by asterisk

phase can be observed for the sample with Cr-concentration; the peaks associated with this phase are shown in the Fig. 1b and indicated by asterisk. Monoclinic structure space group $P2_1$ was assumed for both samples, and the X-rays data were fitted using the Rietveld method for structural refinements. All the peaks were confirmed as belonging to the compound structure, showing very small differences between their experimental position from the measurements and the theoretical ones obtained from the fitting. The dots (line) represent the experimental (theoretical) results and the bottom curve represents the difference between the experimental and theoretical patterns. Also in the figure we have identified the principal peaks of the (−211), (220), (211), and (031) planes that characterize the crystalline $SrAl_2O_4$ structure, according to the registers in the International Centre for Diffraction Data (ICDD) database (JCPDS 74-0794). The lattice parameter

constants resulted $a \approx 8.44(4)$ Å, $b \approx 8.82(1)$ Å, and $c \approx 5.15(8)$ Å, $\beta \approx 93.4°$, with no measurable change in the cell volume. The crystal structure of $SrAl_2O_4$ is derivative of the stuffed tridymite structure, in which all of the Si^{4+} is replaced by Al^{3+} and the charge compensating cation Sr^{2+} occupy the large open channels in the framework. This structure is less regular compared to the hexagonal structure of $SrAl_2O_4$ [18, 19]. In fact, there are two different forms for this compound: a monoclinic form at room temperature and, above 1,000 K, a hexagonal structure. In space group $P2_1$ the triad axis of the hexagonal phase ($P6_3$) is eliminated, which involves a reduction in the symmetry of the trigonally distorted rings and results in the formation of three twin domains. Figure 2 shows the monoclinic structure of $SrAl_2O_4$ projected on (100) plan.

The emission spectra of $SrAl_2O_4$ doped with 1.0 at% Cr^{3+} at room temperature are shown in Fig. 3 for two different Argon excitation lines: (a) 488 nm and (b) 514 nm. Both spectra consist of a broad band beginning in the red region and quenching in the near infrared region and with its barycenter at approximately 855 nm. This broad band can be associated to the ${}^4T_2\ ({}^4F) \rightarrow {}^4\ A_2\ ({}^4F)$ spin-allowed electronic transition of Cr^{3+} ions at strong crystal-field sites. Another characteristic in the emission spectra is a weaker structure, located at 798 nm, and attributed to ${}^2E\ ({}^2G) \rightarrow {}^4\ A_2\ ({}^4F)$ electronic transition. These assignments are characteristic of oxide materials doped with Cr^{3+} ions [20–24]. In our results, the ${}^2E\ ({}^2G) \rightarrow {}^4\ A_2\ ({}^4F)$ transition is more pronounced when the sample is excited at 488 nm. In general, it is characterized by two narrow fluorescent structures, corresponding to the R_1 and R_2 lines. These lines are identified as transitions from the lower and upper levels of the ${}^2E$ level,

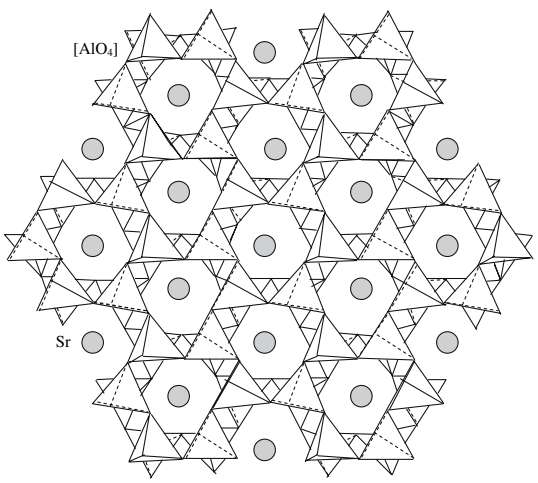

Fig. 2 Monoclinic structure of $SrAl_2O_4$ ($P2_1$) projected onto (100) with the linkage patterns of the [AlO_4] tetrahedra. The solid lines show the unit cells and closed gray circles indicate Sr atoms

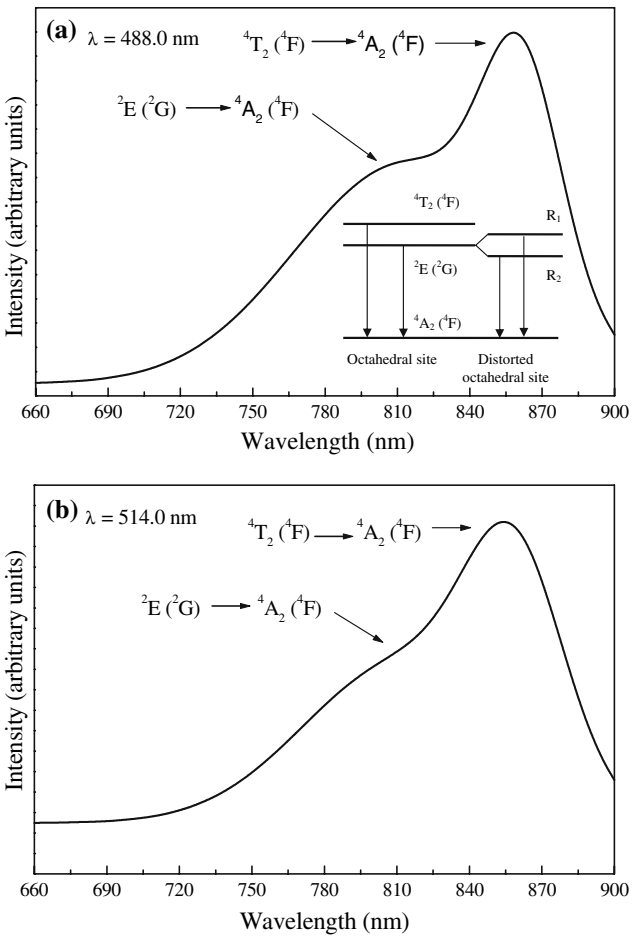

Fig. 3 Emission spectra of Cr-doped $SrAl_2O_4$ at room temperature and excited by an Ar laser in two different lines: (**a**) $\lambda = 488.0$ nm and (**b**) $\lambda = 514.0$ nm. The inset shows a schematic energy levels diagram with the optical transitions for emission spectra. R_1 and R_2 lines are not distinguished at room temperature due to ${}^4T_2\ ({}^4F) \rightarrow {}^4\ A_2\ ({}^4F)$ emission band

respectively, when the Cr^{3+} ions are located in distorted octahedral symmetry sites. Emission spectra of Cr^{3+} ions in full octahedral symmetry are characterized by a single line with attendant vibronic sideband and relatively long radiative lifetime. However, as mentioned in the last section, $SrAl_2O_4$ has a less regular structure and it is more probable that Cr^{3+} ions occupy distorted sites in the lattice, generating the two R lines in the spectrum. At room temperature, it is so difficult to observe R_2 structure because its intensity is weaker than that of the R_1 line and the broader $SrAl_2O_4$:Cr^{3+} luminescence band has covered the weakest R_2 line. Similar results have been previously reported for oxide compounds doped with Cr^{3+} ions at room temperature [1, 25–28]. The fluorescence lifetimes of the ${}^2E$ and ${}^4T_2$ structures at 798 and 855 nm are 250 and 140 μs, respectively. The observed lifetime for ${}^2E\ ({}^2G) \rightarrow {}^4\ A_2\ ({}^4F)$ electronic transition is reduced when it is compared with the obtained values of several ms for Cr^{3+} ions in

strongly distorted environments [28]. A more detailed discussion about this point is given in the end of the section.

Figure 4 shows the excitation spectrum for the same sample at room temperature. The excitation was scanned from 430 to 680 nm and the emission was fixed at 800 nm in order to avoid any pertubation from stray light. Moreover, it is not observed important changes in the excitation spectrum when the monitoring wavelength is altered from 780 to 880 nm. The excitation spectrum presents the two traditional bands for Cr^{3+} ions in octahedral coordination. The band located in the lower energy region is identified as $^4A_2\ (^4F) \rightarrow ^4\ T_2\ (^4F)$ excitation band and the other one, in the higher energy region, is associated with the $^4A_2\ (^4F) \rightarrow ^4\ T_1\ (^4F)$ transition. These broad bands reflect electronic transitions accompanied by the simultaneous annihilation of one or several phonons. In this spectrum, it is not correct to locate the $^4A_2(^4F) \rightarrow ^4\ T_2(^4F)$ and $^4A_2\ (^4F) \rightarrow ^4\ T_1\ (^4F)$ transitions for Cr^{3+} sites from the peak positions, because a large error is made on the position of vibronically coupled levels. In this case, we have determined the exact position of these transitions from analysis mathematical software that fits the excitation spectrum. Hence, the $^4A_2\ (^4F) \rightarrow ^4\ T_1\ (^4F)$ excitation bands have their barycenter at 623 and 463 nm, respectively. The following analysis is based on crystal-field theory and a fuller description about this method is given in many review papers [28–31]. From the position of the excitation bands and ^2E level in the emission spectra, one can evaluate the usual spectroscopic parameters, the Dq crystal-field parameter and the Racah parameters B and C, for Cr^{3+} sites. For this purpose, it were used the following expressions given by the Tanabe-Sugano energy matrices for a d^3 configuration [32],

$$\mathrm{E}[^4A_2\ (^4F) \rightarrow ^4\ T_2\ (^4F)] = 10\ Dq \tag{1}$$

$$B = 0.33(2v_1 - v_2)\delta/\ (9v_1 - 5v_2) \tag{2}$$

$$\mathrm{E}[^2E(^2G) \rightarrow ^4\ A_2(^4F)] = 3.05C + 7.9B - 1.8\ B^2/Dq \tag{3}$$

where v_1 and v_2 are the energy values at the barycenters of the $^4T_2\ (^4F)$ and $^4T_1\ (^4F)$ excitation bands, respectively, and δ is the energy difference between the barycenters of these two bands. The Racah C parameter was determined from the $^2E\ (^2G) \rightarrow ^4\ A_2\ (^4F)$ emission but this induces a small error, inferior to 2%. In general, one must use the Fano antiresonances [33] between the $^4A_2\ (^4F) \rightarrow ^4\ T_2\ (^4F)$ excitation band and $^2E\ (^2G)$ or $^2T_1\ (^2G)$ levels. These antiresonances are characterized by singularities, small dips, in the excitation or absorption spectra in the lower energy side of the $^4T_2\ (^4F)$ band. Nevertheless, these dips are not observed in the excitation spectrum and it was chosen the position of the $^2E\ (^2G)$ level to calculate this parameter.

Using the above equations, the crystal-field parameter Dq and Racah parameters B and C obtained for Cr^{3+} ions in $SrAl_2O_4$ were 1,605, 533, and 2,832 cm^{-1}, respectively. These are typical values for oxide compounds doped with Cr^{3+} ions. One can be also verified that the value for Dq/B ratio for Cr^{3+} sites in this compound is 3.0. In d^3 configuration the lowest exciting level can be ^2E or $^4T_2$. It depends on the environmental influence of the corresponding matrix. That is, when $Dq/B > 2.3$, Cr^{3+} ions are located in sites submitted a strong crystal field and, consequently, the lowest exciting level is ^2E. In the contrary case, $Dq/B < 2.3$, the lowest exciting level is $^4T_2$ and Cr^{3+} sites are influenced by a weak or intermediate crystal field. The obtained value shows that $SrAl_2O_4$:Cr^{3+} is a strong crystal-field matrix.

In $SrAl_2O_4$, the strontium ions are in the channels, which are formed by $[AlO_4]^{5-}$ tetrahedral, and form chains in the structure. Strontium ions are coordinated by nine oxygen ions and this site is more regular than the Al^{3+} site [18]. On the other hand, Cr^{3+} ions prefer to replace substitutionally the Al^{3+} ions because they have the same valence and their ionic radii are comparable (0.57 nm for Al^{3+} ion and 0.69 for Cr^{3+} ion). So, one must expect that Cr^{3+} ions substitute the Al^{3+} ions in tetrahedral coordination. However, the Cr^{3+} ion is almost always found in octahedral coordination, but $[AlO_4]^{5-}$ has a tetrahedral coordination. As the doped samples present a green color, indicating the presence of trivalent chromium in octahedral

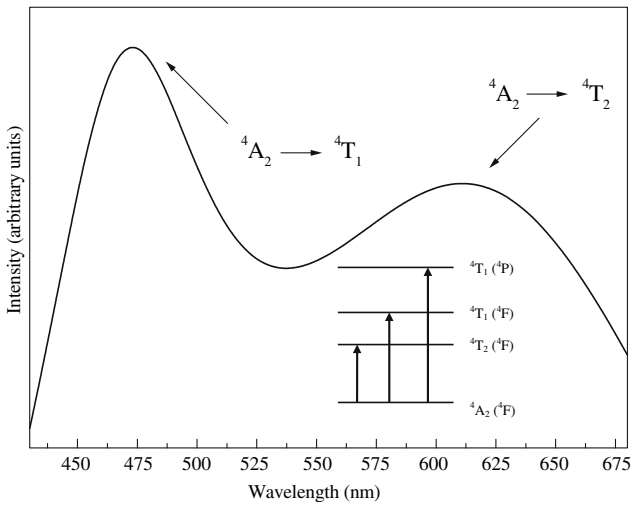

Fig. 4 Excitation spectrum of Cr-doped $SrAl_2O_4$ at room temperature for the emission at 800 nm. This spectrum exhibits two main bands corresponding to the transitions from the $^4A_2\ (^4F)$ to the $^4T_2\ (^4F)$ and $^4T_1\ (^4F)$ levels. The inset shows a simplified diagram with these optical absorption transitions and the $^4A_2\ (^4F) \rightarrow ^4\ T_1\ (^4P)$ transition, which is not observed in the excitation spectrum due to the experimental system response

coordination, we have suggested two occupation possibilities for Cr^{3+} ions in the $SrAl_2O_4$ matrix. Firstly, this unusual tetrahedral coordination environment can tend strongly to transform into the more stable 6-fold coordination geometry by binding two tetrahedrons during the doped sample preparation. In this case, Cr^{3+} ion occupies the central position of the distorted octahedral coordination. X-ray diffraction results, see Fig. 1b, show a small presence of a secondary phase, which can justify this hypothesis. Generally, a great distortion like this one gives a lifetime for $^2E\ (^2G) \rightarrow {}^4A_2\ (^4F)$ electronic transition about few milliseconds but it was measured 250 μs. Although this consideration, a strong coupling with the phonon spectrum of the host compound can decrease the lifetime of this electronic transition. A second possibility is the substitution of Sr^{2+} cations by Cr^{3+} ions because this site is large and presents an approximate octahedral coordination. In this case, a charge compensation ion, probably Cr^{2+}, must be present in the $SrAl_2O_4$ lattice. This could explain the reduction in the lifetime of the $^2E\ (^2G) \rightarrow {}^4A_2\ (^4F)$ transition associated to the energy transfer from Cr^{3+} ions to Cr^{2+} ions and the unknown small phase in the X-ray measurements. Additional measurements will be performed in order to determine exactly the origin of the Cr^{3+} emission centers.

Conclusions

In this work, $SrAl_2O_4$ compound with 1.0 at.% of Cr^{3+} has been investigated by optical spectroscopy at room temperature for the first time. The initial results showed that crystal-field theory can explain the observed optical transitions in the emission spectra and the spectroscopic parameters are typical of Cr^{3+} ions in octahedral coordination. However, the exact origin of the emission in the excitation and emission spectra are not still well-identified and can be related to other symmetry of the Cr^{3+} site or other valence of chromium in this structure. Consequently, time-resolved fluorescence spectroscopy and measurements at low temperatures are in progress in order to investigate the possible emission from different centers in this material and the quantum efficiency of the emission. Moreover, optical measurements will be extended to the 2.0 μm wavelength range to verify a possible emission of Cr^{2+} centers.

Acknowledgements The work described here was financially supported by the research national agencies FINEP and CNPq and by FAPERJ, the Rio de Janeiro State research agency.

References

1. Shen YR, Grinberg M, Barzowska J, Bray KL, Hanuza J, Deren PJ (2006) J Luminesc 116:1
2. Sosman LP, da Fonseca RJM, Dias Tavares Jr A, Abritta T (2006) Ceramica 52:205
3. Sosman LP, da Fonseca RJM, Dias Tavares Jr A, Nakaema MKK, Bordallo HN (2006) J Fluoresc 16:317
4. Liu Y, Xu C-N (2003) J Phys Chem B 107:3991
5. Katsumata T, Nabae T, Sasajima K, Matsuzawa T (1998) J Cryst Growth 183:361
6. Jestin Lenus A, Govinda Rajan K, Yousuf M, Sornadurai D, Purniah B (2002) Mater Lett 54:70
7. Tang T-P, Lee C-M, Yen F-C (2006) Ceram Int 32:665
8. Clabau F, Rocquefelt X, Le Mercier T, Deniard P, Jobic S, Whangbo M-H (2006) Chem Mater 18:3212
9. Xu C-N, Yamada H, Wang X, Zheng X-G (2004) Appl Phys Lett 84:3040
10. Pellé F, Aitasalo T, Lastusaari M, Niittykoski J, Hölsä J (2006) J Luminesc 119–120:64
11. Zhong R, Zhang J, Zhang X, Lu S, Wang X-J (2006) J Luminesc 119–120:327
12. Yang P, Lü MK, Song CF, Liu SW, Xu D, Yuan DR, Cheng XF (2003) Opt Mater 24:575
13. Sosman LP, da Fonseca RJM, Dias Tavares Jr A, Barthem RB, Abritta T (2007) J Phys Chem Solids 68:22
14. Bordallo HN, Henning RW, Sosman LP, da Fonseca RJM, Dias Tavares Jr A, Hanif KM, Strouse GF (2001) J Chem Phys 115:4300
15. Bordallo HN, Wang X, Hanif KM, Strouse GF, da Fonseca RJM, Sosman LP, Dias Tavares Jr A (2002) J Phys: Condens Matter 14:12383
16. da Fonseca RJM, Dias Tavares Jr A, Silva PS, Abritta T, Khaidukov NM (1999) Solid State Commun 110:519
17. Demtröder W (1982) Laser spectroscopy, Springer-Verlag, pp 557–560
18. Fukuda K, Fukushima K (2005) J Solid State Chem 178:2709
19. Poort SHM, Blokpoel WP, Blasse G (1995) Chem Mater 7:1547
20. Happek U, Salley GM (2007) J Luminesc 125:104
21. Qiao B, Tang ZL, Zhang ZT, Chen L (2007) Mater Lett 61:401
22. Su F, Deng Z (2006) J Fluoresc 16:43
23. Gao M, Kapphan S, Pankrath R (2000) J Phys Chem Solids 61:1959
24. Tanner PA (2004) Chem Phys Lett 388:488
25. Ryba-Romanowski W, Golab S, Pisarski WA, Dominiak-Dzik G, Palatnikov MN, Sidonov NV, Kallinikov VT (1997) Appl Phys Lett 70:2505
26. Xia H, Wang J, Wang H, Zhang J, Zhang Y, Xu T (2006) Rare Earths 25:51
27. Glynn TJ, Imbusch GF, Walker G (1991) J Luminesc 48–49:541
28. Kück S (2001) Appl Phys B 72:515
29. Marfunin AS (1979) Physics of minerals and inorganic materials: an introduction, Springer-Verlag, pp 209–213
30. Blasse G (1988) Prog Solid State Chem 18:79
31. Grinberg M (1993) J Luminesc 54:396
32. Tanabe Y, Sugano S (1954) J Phys Soc Japan 9:753
33. Fano U (1961) Phys Rev 124:1866